JOURNAL OF AGRICULTURAL AND FOOD CHEMISTRY

Quantitative Structure–Antifungal Activity Relationships of Some Benzohydrazides against *Botrytis cinerea*

JOSÉ L. REINO,[†] LIANE SAIZ-URRA,[‡] ROSARIO HERNÁNDEZ-GALÁN,[†] VICENTE J. ARÁN,[§] PETER B. HITCHCOCK,[||] JAMES R. HANSON,[||] MAYKEL PEREZ GONZALEZ,[‡,⊥,#] AND ISIDRO G. COLLADO*,[†]

Departamento de Química Orgánica, Facultad de Ciencias, Universidad de Cádiz, Apartado 40, 11510 Puerto Real, Cádiz, Spain, Chemical Bioactive Center, Central University of Las Villas, Santa Clara, Villa Clara, C.P. 54830, Cuba, Instituto de Química Médica, Consejo Superior de Investigaciones Científicas, c/ Juan de la Cierva, 3, 28006 Madrid, Spain, Department of Chemistry, University of Sussex, Brighton, Sussex, BN1 9QJ, United Kingdom, and Service Unit, Experimental Sugar Cane Station "Villa Clara-Cienfuegos", Ranchuelo, Villa Clara, C.P. 53100, Cuba

Fourteen benzohydrazides have been synthesized and evaluated for their in vitro antifungal activity against the phytopathogenic fungus *Botrytis cinerea*. The best antifungal activity was observed for the *N*′,*N*′-dibenzylbenzohydrazides **3b**−**d** and for the *N*-aminoisoindoline-derived benzohydrazide **5**. A quantitative structure−activity relationship (QSAR) study has been developed using a topological substructural molecular design (TOPS-MODE) approach to interpret the antifungal activity of these synthetic compounds. The model described 98.3% of the experimental variance, with a standard deviation of 4.02. The influence of an ortho substituent on the conformation of the benzohydrazides was investigated by X-ray crystallography and supported by QSAR study. Several aspects of the structure−activity relationships are discussed in terms of the contribution of different bonds to the antifungal activity, thereby making the relationships between structure and biological activity more transparent.

KEYWORDS: Benzohydrazides; crop protection agents; *Botrytis cinerea*; antifungal activity; QSAR; spectral moments

INTRODUCTION

Botrytis species include some serious fungal plant pathogens, which are implicated in many diseases affecting flowers, fruits, cereals, legumes, and other vegetables. In particular, *Botrytis cinerea* Pers. ex Fr. attacks economically important crops such as carrots, grapes, lettuce, strawberries, and tobacco, producing various leaf spot diseases and powdery gray mildews (*1*).

Following the discovery of the systemic antifungal properties of carboxamides, several compounds, including fenfuram, carboxin, and oxycarboxin, were synthesized and introduced as agricultural fungicides (*2*). Within this group, the benzanilide fungicides such as benodanil (**1**), flutolanil, mebenil, mepronil, salicylanilide, and tecloftalam were found to exhibit a wide spectrum of activity against pathogens such as *Rhizoctonia solani* and various *Typhula*, *Corticium*, and *Gymnosporangium* species (*3*, *4*).

Hydrazides, which are the subject of this study, are known to exhibit various biological activities including tuberculostatic (*5*, *6*), antibacterial (*7*), anticonvulsant (*8*), and antifungal activities (*9*).

Quantitative structure−activity relationships (QSAR) are widely used in the search for new and better compounds with a specific biological activity. This methodology uses molecular descriptors reflecting the structure of the molecules, which can then be used in the development of predictive models. This methodology gives rise to cost savings by reducing laboratory resources used and research time required. Another characteristic of this technique is its potential to analyze theoretical aspects of the role of specific molecules or molecule fragments in a certain biological activity.

In spite of the fact that many QSAR studies have been reported about antifungal activity, a small number of limited studies has been conducted aimed at exploring the use of QSAR techniques in the rational search for new fungicides against *B. cinerea* (*10*−*13*). It is important to highlight that the largest QSAR unified model for antifungal compounds reported up to date does not include *B. cinerea* among the strains taken into account (*14*).

Two- and three-dimensional molecular descriptors have been widely used in QSAR research. However, these descriptors have

* To whom correspondence should be addressed. Tel: 34 956 016371. Fax: 34 956 016193. E-mail: isidro.gonzalez@uca.es.
[†] Universidad de Cádiz.
[‡] Central University of Las Villas.
[§] Consejo Superior de Investigaciones Científicas.
[||] University of Sussex.
[⊥] Experimental Sugar Cane Station.
[#] Universidad Santiago de Compostela.

10.1021/jf0704211 CCC: $37.00
Published on Web 06/02/2007

not previously been used in the development of models to predict fungicidal activity against *B. cinerea*.

Additionally, our ready access to compounds containing a benzohydrazide skeleton analogous to the structure of the commercial fungicide benodanil (**1**) and our interest in the control of *B. cinerea* has prompted us to undertake the synthesis of several *N*′,*N*′-disubstituted benzohydrazides.

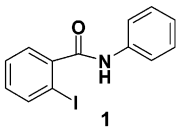

1

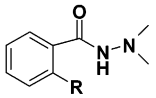

R=H 2a
R=F 2b
R=Cl 2c
R=I 2d

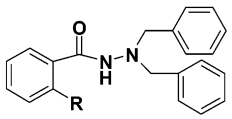

R=H 3a
R=Cl 3b
R=I 3c
R=Me 3d

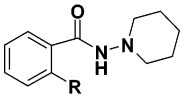

R=H 4a
R=F 4b
R=Cl 4c
R=I 4d
R=OMe 4e

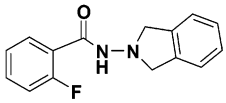

5

In this paper, we describe both the synthesis and the results of our tests on the fungistatic activity of these benzohydrazides. Several aspects of the stereochemical relationship between their structure and biological activity are discussed. Another aim is to develop a predictive model of the antifungal activity for this group of compounds and to determine the contribution made by several structural fragments to the relationship, between structure and biological activity.

MATERIALS AND METHODS

We prepared a series of substituted benzohydrazides **2a**−**d**, **3a**−**d**, **4a**−**e**, and **5** by acylating the hydrazines with the corresponding acid chlorides (*15*). These compounds were then screened for antifungal activity at 50, 100, and 200 μg/mL against the phytopathogen *B. cinerea*. The reference substance, benodanil (**1**) (50 μg/mL), was included in all tests as a positive control. The X-ray crystal structures of compounds **3a**,**b** were determined.

General Experimental Procedures. Melting points were determined with a Reichert−Jung Thermovar hot-stage microscope. ^{1}H (300 MHz) and ^{13}C (75, 100, or 125 MHz) NMR spectra were recorded on Varian Inova 300, Varian Inova 400, or Varian Unity 600 spectrometers. Chemical shifts are reported in ppm from TMS (δ scale) but were measured against the solvent signal ($CDCl_3$: $\delta_H = 7.24$; $\delta_C = 77.0$). *Z*/*E* rotamer ratios of hydrazides were determined using the relative integrals for the $N[CH_n]_2$ signals corresponding to each isomer in the ^{1}H NMR spectra. δ_C Values reported in the literature for 2-substituted benzoic acids (*16*) and esters (*17*) were consulted for the assignment of ^{13}C NMR spectra. Electron impact (EI) mass spectra were obtained at 70 eV on a Hewlett-Packard 5973 MSD spectrometer. Microanalyses were performed by the Departamento de Análisis, Centro de Química Orgánica "Manuel Lora Tamayo", CSIC (Madrid, Spain).

Preparation of Substituted Benzohydrazides. The preparation of hydrazides **2a**−**c**, **4b**,**c**, and **5** has been previously described (*15*). Hydrazides **2d**, **4a**,**d**,**e**, and **3a**−**d** were prepared by acylation of the corresponding hydrazines with acid chlorides using, respectively, triethylamine or sodium hydrogencarbonate as bases (previously reported methods A_1 and A_2) (*15*).

2-Iodo-*N*′,*N*′-dimethylbenzohydrazide (2d). Yield, 75% (method A_1); mp 155−157 °C (toluene). IR (KBr) ν_{max}: 3217 (NH), 1650 (CO) cm^{-1}. ^{1}H NMR ($CDCl_3$): δ = 7.86−6.98 (m, 4 H, aromatic H, *Z* and *E* rot.), 6.59 (br s, *E* rot.) and 6.48 (br s, *Z* rot.) (1 H, NH), 2.71 (s, *Z* rot.) and 2.50 (s, *E* rot.) (6 H, CH_3) (*Z* rot./*E* rot. ratio: 78/22). ^{13}C NMR ($CDCl_3$): δ = 172.5 (*E* rot.) and 167.0 (*Z* rot.) (CO), 142.3 (*E* rot.) and 140.7 (*Z* rot.) (C-1), 139.4 (*Z* rot.) and 138.9 (*E* rot.) (C-3), 131.0 (*Z* rot.) and 129.9 (*E* rot.) (C-4), 128.3 (*Z* rot.), 128.0 (*Z* rot.), 127.4 (*E* rot.) and 126.3 (*E* rot.) (C-5, −6), 92.6 (*Z* rot.) and 91.4 (*E* rot.) (C-2), 48.4 (*E* rot.) and 47.1 (*Z* rot.) (CH_3). EI MS: *m*/*z* (%) = 290 (M^+, 10), 248 (89), 247 (79), 231 (100), 203 (45), 105 (14), 76 (40), 59 (77). $C_9H_{11}IN_2O$ (290.10) calcd: C, 37.26; H, 3.82; N, 9.66; I, 43.74. Found: C, 36.98; H, 4.01; N, 9.82; I, 43.50%.

***N*′,*N*′-Dibenzylbenzohydrazide (3a).** Yield, 89% (method A_2); mp 168−170 °C (EtOH); lit. (*18*), 169 °C.

***N*′,*N*′-Dibenzyl-2-chlorobenzohydrazide (3b).** Yield, 89% (method A_2); mp 125−127 °C (2-PrOH). IR (KBr) ν_{max}: 3216 (NH), 1658 (CO) cm^{-1}. ^{1}H NMR ($CDCl_3$): δ = 7.50−6.28 (m, 15 H, aromatic H and NH, *Z* and *E* rot.), 4.30 (s, *Z* rot.) and 3.78 (s, *E* rot.) (4 H, CH_2) (*Z* rot./*E* rot. ratio: 78/22). ^{13}C NMR ($CDCl_3$): δ = 171.2 (*E* rot.) and 166.0 (*Z* rot.) (CO), 137.2 (*Z* rot.) and 135.3 (*E* rot.) (C-1′′), 135.6 (*E* rot.) and 134.3 (*Z* rot.) (C-1), 131.0 (*Z* rot.) and 129.6 (*E* rot.) (C-4), 130.9 (*Z* rot.) and 129.92 (*E* rot.) (C-2), 129.90 (*Z* rot.) and 128.9 (*E* rot.) (C-3), 129.8 (*E* rot.), 129.3 (*Z* rot.), 128.4 (*E* rot.) and 128.3 (*Z* rot.) (C-2′′, -3′′, -5′′, -6′′), 129.2 (*Z* rot.) and 128.0 (*E* rot.) (C-6), 127.7 (*E* rot.) and 127.4 (*Z* rot.) (C-4′′), 126.7 (*Z* rot.) and 126.1 (*E* rot.) (C-5), 61.5 (*E* rot.) and 59.4 (*Z* rot.) [C-1′ (CH_2)]. EI MS: *m*/*z* (%) = 350 (M^+, 0.4), 259 (14), 211 (28), 196 (53), 195 (66), 194 (56), 156 (41), 139 (55), 111 (22), 91 (100). $C_{21}H_{19}ClN_2O$ (350.85) calcd: C, 71.89; H, 5.46; N, 7.98; Cl, 10.10. Found: C, 72.02; H, 5.70; N, 8.08; Cl, 10.21%.

***N*′,*N*′-Dibenzyl-2-iodobenzohydrazide (3c).** Yield, 90% (method A_2); mp 139−141 °C (EtOH). IR (KBr) ν_{max}: 3218 (NH), 1654 (CO) cm^{-1}. ^{1}H NMR ($CDCl_3$): δ = 7.86−6.24 (m, 15 H, aromatic H and NH, *Z* and *E* rot.), 4.31 (s, *Z* rot.) and 3.81 (s, *E* rot.) (4 H, CH_2) (*Z* rot./*E* rot. ratio: 80/20). ^{13}C NMR ($CDCl_3$): δ = 173.2 (*E* rot.) and 168.3 (*Z* rot.) (CO), 141.7 (*E* rot.) and 140.4 (*Z* rot.) (C-1), 139.7 (*Z* rot.) and 138.6 (*E* rot.) (C-3), 137.2 (*Z* rot.) and 135.1 (*E* rot.) (C-1′′), 131.0 (*Z* rot.) and 129.8 (*E* rot.) (C-4), 129.8 (*E* rot.), 129.3 (*Z* rot.), 128.4 (*E* rot.) and 128.3 (*Z* rot.) (C-2′′, -3′′, -5′′, -6′′), 127.9 (*Z* rot.), 127.7 (*Z* rot.), 127.5 (*E* rot.) and 127.2 (*E* rot.) (C-5, −6), 127.8 (*E* rot.) and 127.4 (*Z* rot.) (C-4′′), 92.6 (*Z* rot.) and 91.5 (*E* rot.) (C-2), 61.3 (*E* rot.) and 59.4 (*Z* rot.) [C-1′ (CH_2)]. EI MS: *m*/*z* (%) = 442 (M^+, 0.4), 351 (14), 248 (54), 231 (55), 211 (31), 203 (24), 196 (58), 195 (71), 194 (47), 118 (10), 105 (15), 91 (100). $C_{21}H_{19}IN_2O$ (442.30) calcd: C, 57.03; H, 4.33; N, 6.33; I, 28.69. Found: C, 57.21; H, 4.22; N, 6.51; I, 28.91%.

***N*′,*N*′-Dibenzyl-2-methylbenzohydrazide (3d).** Yield, 91% (method A_2); mp 126−128 °C (2-PrOH). IR (KBr) ν_{max}: 3226 (NH), 1665 (CO) cm^{-1}. ^{1}H NMR ($CDCl_3$): δ = 7.50−6.30 (m, 15 H, aromatic H and NH, *Z* and *E* rot.), 4.25 (s, *Z* rot.) and 3.69 (s, *E* rot.) (4 H, CH_2), 2.06 (s, *Z* rot.) and 1.89 (s, *E* rot.) (3 H, CH_3) (*Z* rot./*E* rot. ratio: 91/9). ^{13}C NMR ($CDCl_3$): δ = 173.7 (*E* rot.) and 169.2 (*Z* rot.) (CO), 137.3 (*Z* rot.) and 135.2 (*E* rot.) (C-1′′), 136.2 (*Z* rot.) and 134.8 (*E* rot.) (C-2), 135.5 (*E* rot.) and 134.9 (*Z* rot.) (C-1), 130.7 (*Z* rot.) and 130.0 (*E* rot.) (C-4), 129.7 (*Z* rot.) and 128.9 (*E* rot.) (C-3), 129.5 (*E* rot.), 129.2 (*Z* rot.), 128.5 (*E* rot.) and 128.3 (*Z* rot.) (C-2′′, -3′′, -5′′, -6′′), 127.8 (*E* rot.) and 127.5 (*Z* rot.) (C-4′′), 126.7 (*E* rot.) and 126.5 (*Z* rot.) (C-6), 125.4 (*Z* rot.) and 124.5 (*E* rot.) (C-5), 61.8 (*E* rot.) and 59.8 (*Z* rot.) [C-1′ (CH_2)], 19.04 (*Z* rot.) and 18.98 (*E* rot.) (CH_3). EI MS: *m*/*z* (%) = 330 (M^+, 1), 239 (14), 211 (37), 196 (73), 195 (62), 194 (46), 136 (50), 119 (63), 104 (6), 91 (100). $C_{22}H_{22}N_2O$ (330.43) calcd: C, 79.97; H, 6.71; N, 8.48. Found: C, 80.12; H, 6.43; N, 8.28%.

***N*-Piperidinobenzamide (4a).** Yield, 82% (method A_1); mp 197−199 °C (toluene); lit. (*19*), 193−195 °C; lit. (*20*), 198−199 °C.

2-Iodo-*N*-piperidinobenzamide (4d). Yield, 88% (method A_1); mp 147−149 °C (toluene). IR (KBr) ν_{max}: 3212 (NH), 1663 (CO) cm^{-1}. ^{1}H NMR ($CDCl_3$): δ = 7.84−6.98 (m, 4 H, aromatic H, *Z* and *E* rot.), 6.57 (br s, *E* rot.) and 6.40 (br s, *Z* rot.) (1 H, NH), 2.88 (m, *Z* rot.)

Table 1. Antifungal Bioassays of Compounds **2a**–**d**, **3a**–**d**, **4a**–**e**, and **5** against *B. cinerea*

	% inhibition[a]		
compounds	200 μg/mL	100 μg/mL	50 μg/mL
2a	51 ± 2	45 ± 3	24 ± 4
2b	32 ± 1	22 ± 1	12 ± 0
2c	33 ± 2	0 ± 0	0 ± 0
2d	33 ± 1	28 ± 2	19 ± 1
3a	44 ± 3	42 ± 2	10 ± 0
3b	86 ± 2	42 ± 2	31 ± 1
3c	82 ± 1	50 ± 2	27 ± 1
3d	88 ± 2	55 ± 2	48 ± 4
4a	45 ± 1	43 ± 1	37 ± 3
4b	51 ± 1	51 ± 6	46 ± 1
4c	57 ± 3	40 ± 2	36 ± 4
4d	46 ± 2	42 ± 1	33 ± 1
4e	51 ± 1	47 ± 1	38 ± 1
5	91 ± 1	50 ± 1	42 ± 1

[a] Results are the means of at least three independent experiments conducted in triplicate.

and 2.70 (br s, *E* rot.) (4 H, 2′-, 6′-H), 1.75 (m), 1.42 (m) and 1.25 (m) (6 H, 3′-, 4′-, 5′-H, *Z* and *E* rot.) (*Z* rot./*E* rot. ratio: 82/18). ^{13}C NMR ($CDCl_3$): δ = 172.6 (*E* rot.) and 166.7 (*Z* rot.) (CO), 142.3 (*E* rot.) and 140.9 (*Z* rot.) (C-1), 139.4 (*Z* rot.) and 138.7 (*E* rot.) (C-3), 131.0 (*Z* rot.) and 129.7 (*E* rot.) (C-4), 128.4 (*Z* rot.), 128.0 (*Z* rot.), 127.2 (*E* rot.) and 126.5 (*E* rot.) (C-5, −6), 92.7 (*Z* rot.) and 91.6 (*E* rot.) (C-2), 57.7 (*E* rot.) and 56.7 (*Z* rot.) (C-2′, −6′), 25.1 (*Z* and *E* rot., C-3′, −5′), 23.1 (*Z* rot.) and 22.7 (*E* rot.) (C-4′). EI MS: *m*/*z* (%) = 330 (M^+, 3), 325 (7), 296 (4), 286 (11), 248 (45), 247 (30), 231 (43), 210 (11), 203 (30), 186 (19), 105 (11), 99 (100), 83 (58), 76 (31). $C_{12}H_{15}IN_2O$ (330.17) calcd: C, 43.65; H, 4.58; N, 8.48; I, 38.44. Found: C, 43.75; H, 4.52; N, 8.28; I, 38.21%.

2-Methoxy-*N*-piperidinobenzamide (4e). Yield, 77% (method A_1); mp 92−94 °C (cyclohexane). IR (KBr) ν_{max}: 3325 (NH), 1663 (CO) cm^{-1}. ^{1}H NMR ($CDCl_3$): δ = 8.50 (br s, 1 H, NH), 8.15 (dd, J_o = 7.7, J_m = 1.6, 1 H, 6-H), 7.40 (m, 1 H, 4-H), 7.04 (m, 1 H, 5-H), 6.93 (d, J_o = 8.1, 1 H, 3-H), 3.93 (s, 3 H, CH_3), 2.89 (br t, J = 5.3, 4 H, 2′-, 6′-H), 1.72 (m, 4 H, 3′-, 5′-H), 1.43 (m, 2 H, 4′-H) (100% of *Z* rot.). ^{13}C NMR ($CDCl_3$): δ = 163.0 (CO), 156.9 (C-2), 132.5 (C-4), 132.2 (C-6), 121.3 (C-1, -5), 111.2 (C-3), 56.7 (C-2′, -6′), 55.8 (CH_3), 25.2 (C-3′, -5′), 23.4 (C-4′) (100% of *Z* rot.). EI MS: *m*/*z* (%) = 234 (M^+, 3), 217 (3), 203 (2), 190 (10), 152 (58), 135 (100), 105 (12), 99 (51), 92 (20), 84 (56), 77 (38). $C_{13}H_{18}N_2O_2$ (234.30) calcd: C, 66.64; H, 7.74; N, 11.96. Found: C, 66.86; H, 7.70; N, 12.18%.

Microorganism and Antifungal Assays. The isolate used in this work, *B. cinerea* 2100, was obtained from the "Centro Español de Cultivos Tipos" (CECT), Facultad de Biología, Universidad de Valencia (Spain), where this strain is on deposit. Bioassays were performed by measuring radial growth inhibition on an agar medium in a Petri dish. The test compound was dissolved in acetone to give final compound concentrations ranging from 50 to 200 μg/mL. Solutions of the test compound were added to a glucose−malt−peptone−agar medium (61 g of glucose−malt−peptone−agar per liter, pH 6.5−7.0). The final acetone concentration was identical in both the control and the test cultures. The medium was poured into sterile plastic Petri dishes measuring 9 cm in diameter, and a mycelial disc of *B. cinerea* cut from an actively growing culture and measuring 5 mm in diameter was placed at the center of the agar plate. The radial growth inhibition was measured for 6 days. Percentages of growth inhibition were calculated by comparing the mean value of the diameters of the mycelia in the test plates with that of the untreated control plates. Each determination assay was conducted in triplicate and repeated at least three times.

X-ray Crystal Data and Structure Determination of *N*′,*N*′-Dibenzylbenzohydrazide (3a). Crystallographic data (**Table 2**) have been deposited at the Cambridge Crystallographic Data Centre, CCDC No. 251521.

***N*′,*N*′-Dibenzyl-2-chlorobenzohydrazide (3b).** Crystallographic data (**Table 3**) have been deposited at the Cambridge Crystallographic Data Centre, CCDC No. 251522.

Table 2. Crystal and Structure Refinement for Compound **3a**

empirical formula	$C_{21}H_{20}N_2O$	
formula weight	316.39	
temperature	173(2) K	
wavelength	0.71073	
crystal system	monoclinic	
space group	$P2_1/c$ (no. 14)	
unit cell dimensions	a = 9.9014(3) Å	α = 90°
	b = 17.0048(6) Å	β = 96.307(2)°
	c = 10.0709(3) Å	γ = 90°
volume	1685.39(9) Å^3	
Z	4	
density (calculated)	1.25 mg m^{-3}	
absorption coefficient	0.08 mm^{-1}	
F(000)	672	
crystal size	0.2 × 0.2 × 0.1 mm^3	
θ range for data colletion	3.89–25.02°	
index ranges	$-11 \le h \le 11$,	
	$-20 \le k \le 20$,	
	$-11 \le l \le 11$	
reflections collected	11875	
independent reflections	2943 [R(int) = 0.048]	
reflections with $I > 2\sigma(I)$	2389	
completeness to θ = 25.02°	99.0%	
refinement method	full-matrix least-squares on F^2	
data/restraints/parameters	2943/0/298	
goodness-of-fit on F^2	0.989	
final R indices [$I > 2\sigma(I)$]	R_1 = 0.040, wR_2 = 0.099	
R indices (all data)	R_1 = 0.056, wR_2 = 0.119	
extinction coefficient	0.102(8)	
largest diff peak and hole	0.39 and –0.36 e Å^{-3}	

Table 3. Crystal and Structure Refinement for Compound **3b**

empirical formula	$C_{21}H_{19}ClN_2O$	
formula weight	350.83	
temperature	173(2) K	
wavelength	0.71073	
crystal system	triclinic	
space group	P (no. 2)	
unit cell dimensions	a = 9.6251(3) Å	α = 74.513(2)°
	b = 10.9307(4) Å	β = 85.429(2)°
	c = 17.9455(6) Å	γ = 89.801(2)°
volume	1813.38(11) Å^3	
Z	4	
density (calculated)	1.29 mg m^{-3}	
absorption coefficient	0.22 mm^{-1}	
F(000)	736	
crystal size	0.30 × 0.15 × 0.10 mm^3	
θ range for data colletion	3.73–25.11°	
index ranges	$-11 \le h \le 11$,	
	$-12 \le k \le 13$,	
	$-21 \le l \le 21$	
reflections collected	23862	
independent reflections	6370 [R(int) = 0.081]	
reflections with $I > 2\sigma(I)$	4563	
completeness to θ = 25.02°	98.5%	
refinement method	full-matrix least-squares on F^2	
data/restraints/parameters	6370/0/603	
goodness-of-fit on F^2	1.030	
final R indices [$I > 2\sigma(I)$]	R_1 = 0.051, wR_2 = 0.108	
R indices (all data)	R_1 = 0.085, wR_2 = 0.122	
largest diff peak and hole	0.20 and –0.37 e Å^{-3}	

Molecular Descriptors. *Spectral Moments.* Spectral moments are based on the calculation of the bond matrix, whose theoretical basis has been widely described in previous reports (*21*, *22*). Essentially, the bond matrix is the square and symmetric matrix whose entries are ones or zeros according to whether the corresponding bonds are adjacent or not. The order of this matrix (m) is the number of bonds in the molecular graph, two bonds being adjacent if they have one common atom. The spectral moments of the edge adjacency matrix are defined

as the traces, that is, the sum of the main diagonal of the different powers of such a matrix.

The following steps were followed in applying the above approach to the development of a model for predicting antifungal activity. (i) An adequate training set of chemicals was selected; (ii) the molecular graphs for each of the training set were drawn; (iii) molecular bonds with appropriate weights were differentiated; (iv) the spectral moments of the bond matrix for each molecule in the data set were computed; (v) a QSAR was derived by using multiple regression analysis (MRA); (vi) the predictive performance of the model was assessed employing the leave one out (LOO) and leave group out (LGO) cross-validation methodologies; and (vii) the contribution of the different fragments was ascertained to determine their quantitative contribution to the antifungal activity of the molecules studied.

For the development of the MRA, we used the following expression

$$P = a_0\mu_0 + a_1\mu_1 + a_2\mu_2 + ... + a_k\mu_k + b \quad (1)$$

where P is the activity under study (the percentage of growth inhibition), μ_k is the kth spectral moment, and the a_k values are the coefficients obtained by the regression equation.

Selection of Bond Weights and Calculation of Molecular Descriptors. Hydrophobicity (Hyd), molar refractivity (Mol), and Gasteiger−Marsilli (GM) charge were used as bond weights. The latter is an atomic contribution, and it was transformed into bond contributions, according to eq 2. This transformation has been previously described (*23*)

$$w(i,j) = \frac{w_i}{\delta_i} + \frac{w_j}{\delta_j} \quad (2)$$

where w_i and δ_i are the atomic weight and vertex degree of atom i, respectively. The calculation of the spectral moment descriptors was carried out with Modeslab 1.0 software (*24*). The input of the chemical structures into the Modeslab software was carried out using the familiar SMILES notation. We calculated the first 15 spectral moments ($\mu_1-\mu_{15}$) for each bond weight and the number of bonds in the molecules (μ_0). Because of the nonlinearity of the biological process under study (fungicidal activity), the interactions between μ_0 and μ_1 and with all variables (descriptors) were evaluated. Spectral moments were calculated considering the molecules in the absence of hydrogen atoms.

Computational Strategies. The mathematical model was obtained by means of the MRA as implemented in the STATISTICA software version 6.0 (*25*). The data for the compounds which had been synthesized were that for their biological activities reported for 200 μg/mL and 3 days of observation The most significant parameters were identified from the data set using genetic algorithm (GA) analysis as a variable selection strategy of the descriptors obtained by TOPS-MODE computer software. The GA is a class of methods based on biological evolution rules (*26*−*28*). The first step was to create a population of linear regression models. These regression models mate with one another, mutate, cross over, reproduce, and then evolve through successive generations toward an optimal solution. The particular GA simulation conditions applied here are as follows: 1000 generations, 0.5 for the tradeoff between cross over and mutation parameter, 1 smoothness factor, and 300 model populations.

Analysis of residuals and deleted residuals from the regression equations was used to identify outliers. The statistical significance of the models was determined by examining the squared regression coefficient (R^2), the standard deviation (S), the number of variables, and the Fisher ratio (F).

Orthogonalization of Descriptors. The orthogonalization process of molecular descriptors was introduced by Randić several years ago as a way of improving the statistical interpretation of the model, which had been built by using inter-related indices (*29*−*33*). The main philosophy of this approach is to avoid the exclusion of descriptors on the basis of their collinearity with other variables previously included in the model. The acceptable level of collinearity to avoid is a more subjective issue. In our view, the collinearity of the variables should be as low as possible because inter-relatedness among the different descriptors can result in a highly unstable regression coefficient, making it impossible to know the relative importance of an index and underestimating the utility of the regression coefficient model. The Randić method of orthogonalization has been described in detail in several publications (*29*−*33*).

Validation of the Models. The models obtained were validated by calculating the cross-validated squared regression coefficient (q^2) values. The q^2 values are calculated from the LOO test and from the LGO test, also known as cross-validation.

In the case of LOO, a data point is removed from the set, and the regression is recalculated; the predicted value for that point is then compared to its actual value. This is repeated until each piece of data has been omitted once; the sum of squares of these deletion residuals can then be used to calculate q^2, an equivalent statistic to R^2. In the LGO method, 25% of the data was eliminated every time in 100 different forms. In this way, we ensured that the same group of compounds was not used for every validation. The q^2 values can be considered a measure of the predictive power of a regression equation, whereas R^2 can always be increased artificially by adding more parameters (descriptors), q^2 decreases if a model is overparameterized (*34*), and is therefore a more meaningful summary statistic for QSAR models.

Computation of Bond Contributions. Calculation of the fragment contribution has been described previously (*35*, *36*); we will now provide an overview of the methodology used. Bond contributions to antifungal activity were calculated on the basis of the local spectral moments, which were defined as the diagonal entries of the different powers of the weighted bond matrix

$$\mu_k^T(i) = b_{ii}(T)^k \quad (3)$$

where $\mu_k^T(i)$ is the kth local moment of the bond i, $b_{ii}(T)$ are the diagonal entries of the weighted bond matrix, and T is the type of the bond weight: Std, Dip, and GM.

It is plain to see that the total moments are the sum of the local moments. Consequently, we can substitute eq 3 into the QSAR (eq 4) in such a way that the total contribution of the different bonds in a specific molecule was obtained as follows

$$P = b_o + \sum_k a_k \cdot \mu_k^T \quad (4)$$

These contributions represent the additive features of the property modeled, and they can be expressed as fragment contributions, the sum of the contributions of different bonds that are inside the substructure whose contribution is under examination.

RESULTS AND DISCUSSION

The results of the antifungal activity screening test on *B. cinerea* show that in general the benzohydrazides displayed antifungal activity (see **Table 1**) with compounds **3b**−**d** and **5** being the most active against the fungus. It is worth noting that the most active compounds bear an additional aromatic ring on the nitrogen, *N*′, of the hydrazide group, a fact that lends credence to the idea that a second aromatic nucleus on the benzohydrazide skeleton is necessary for a high degree of activity. Thus, while compound **3b** at 200 μg/mL inhibited growth by 86% after 6 days, compound **3d** inhibited growth by 88, 55, and 48% after 6 days at 200, 100, and 50 μg/mL, respectively. Compound **5** was the most active compound, with a 91% inhibition rate after 6 days at 200 μg/mL. These results also indicate that an ortho substituent on the aromatic ring of the benzoic acid contributes to an increase in the activity, as can be seen from a comparison of the activity of compounds **3a**−**d**.

Previous studies (*37*−*39*) have noted that many hydrazides appear in solution (NMR) as mixtures of *Z* and *E* rotamers because of their restricted rotation around the N−CO bond (**Figure 1**), and this may have an impact on their biological activity. Consequently, we investigated several previously

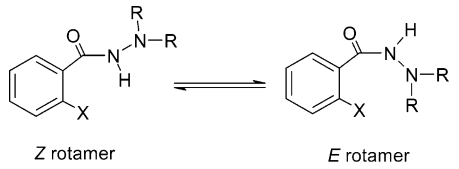

Figure 1. Rotamers *Z* and *E* of benzohydrazides.

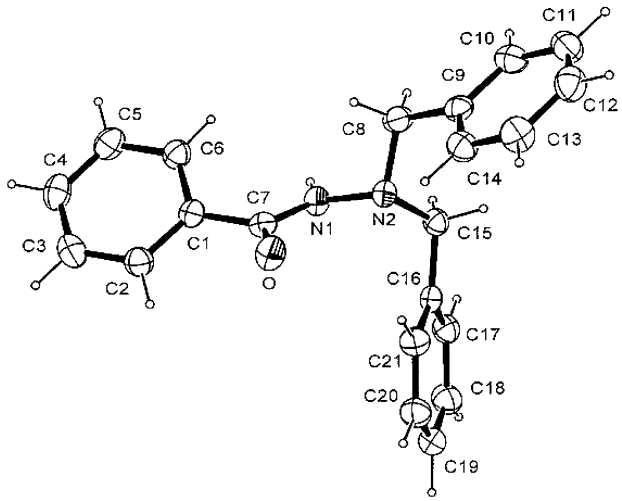

Figure 2. X-ray molecular structure of compound **3a** (ORTEP drawing).

described (*15*) benzohydrazides as well as some reported here for the first time and established the *Z*/*E* rotamer ratios in $CDCl_3$ at room temperature. These ratios were for the 2-fluoro- (**2b**, **4b**, and **5**), 2-chloro- (**2c**, **3b**, and **4c**), 2-iodo- (**2d**, **3c**, and **4d**), 2-methyl- (**3d**), and 2-methoxybenzoic acid (**4e**) derivatives being ca. 93:7, 77:23, 80:20, 91:9, and 100:0, respectively. The signals corresponding to each rotamer were assigned by comparing the NMR spectra of 2-substituted hydrazides with those of unsubstituted benzoic acid derivatives [**2a** (*15*), **3a** (*18*), and **4a** (*19*)] in which only one species, claimed to be the *Z* rotamer in the case of compound **3a** (*39*), can be detected.

A comparison of the X-ray crystal structures (**Figures 2** and **3**) of compounds **3a**,**b** reveals a possible role for the ortho chloro substituent. There are two competing influences on the conformation of the aromatic carboxyhydrazide. On the one hand, there is the tendency for the carbonyl group to become coplanar with the aromatic ring influenced by the conjugation between the two groups. On the other hand, in the crystalline state, there is hydrogen bonding between the amide N−H of one molecule and the carbonyl oxygen of the adjacent molecule. This is favored by twisting the plane of the amide out of the plane of the aromatic ring. In the unsubstituted case, this leads to an angle between the plane of the aromatic ring and the plane of the amide [C(1):C(7):N(1):O(1)] of 35.3° and a hydrogen bond length [d(H···A)] of 2.07 Å. The ortho chloro compound **3b** crystallizes with two independent molecules. However, there is an angle between the planes of 81.5° (60.0° in the second molecule) and a shorter hydrogen bond length (2.01 and 2.00 Å). The angle of the hydrogen bond in **3b** is more near linearity (173 and 174°) as compared to **3a** (161°), indicating the potential for a stronger hydrogen bond in **3b**. Thus, the increased rotation of the carboxyhydrazide brought about by the ortho chlorine facilitates hydrogen bonding between the N−H and another molecule. The biological activity is likely to involve a hydrogen bond interaction between the hydrazide and the fungus. This extra twisting, which is apparent in the crystalline state and

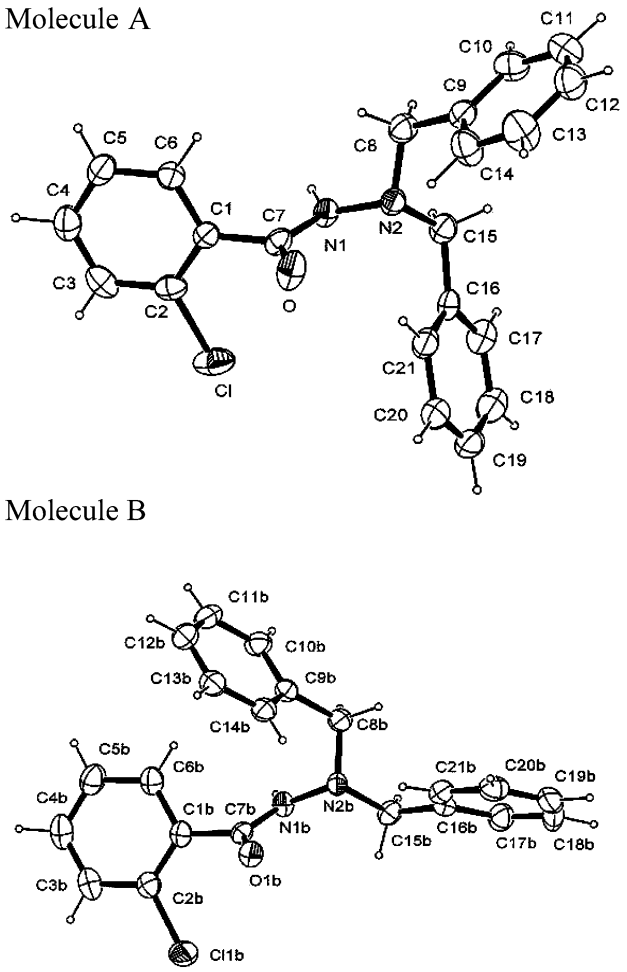

Figure 3. X-ray molecular structure of compound **3b** (ORTEP drawing): molecule A and molecule B.

which makes the amide N−H more readily available for hydrogen bonding, could account for the increase in biological activity.

A QSAR study based on the synthesized compounds was carried out to go deeper into the causes of the increase of the antifungal activity in regard to the chemical structure, emphasizing the bond contributions of the different molecules from the data.

First, three different models were developed taking into account the percentage of the fungal growth inhibition reported at three different concentrations, 200, 100, and 50 μg/mL, to find the one that best describes the antifungal activity of these benzohydrazides through the variables from the TOPS-MODE approach by using GA to select the most significant variables.

Model selection was subjected to the principle of parsimony (*34*). Then, to select the model, a high statistical significance was taken into account in searching for a function with as few parameters as possible. The results of this study are contained in Table 4 where *N* is the number of compounds included in the model, R^2 is the square of the correlation coefficient, *S* is the standard deviation of the regression, *F* is the Fisher ratio, *p* is the significance of the model, and q_{CV-LOO}^2 is the cross-validated squared regression coefficient. The parameter q^2 is used as a criterion of both the robustness and the predictive ability of the model. Many authors consider high q^2 (for instance, $q^2 > 0.5$) as an indicator that the model is predictive (*40*).

It is worth noting that all models are suitable for the prediction of antifungal activity according to the statistical parameters;

Table 4. Models Developed for the Percentage of the Fungal Growth Inhibition at 200, 100, and 50 μg/mL

	model 1	model 2	model 3
variables	$\mu_0\mu_{15}^{GM}$, μ_{11}^{GM}, $\mu_0\mu_1^{GM}$	$\mu_0\mu_6^{Dip}$, $\mu_0\mu_1^{Pol}$, μ_6^{Dip}	$\mu_0\mu_6^{Hyd}$, μ_1^{Pol}, μ_{15}^{Dip}
concentration	200 μg/mL	100 μg/mL	50 μg/mL
N	14	14	14
R^2	0.983	0.900	0.817
S	4.02	4.056	5.749
F	190.355	29.93	14.88
p	$<10^-$	2.6×10^{-5}	5.0×10^{-4}
q_{CV-LOO}^2	0.970	0.785	0.709

Table 5. Models Developed for the Percentage of the Fungal Growth Inhibition at 200, 100, and 50 μg/mL Keeping the Same Variables of the Model at 200 μg/mL

	model 1	model 4	model 5
variables	$\mu_0\mu_{15}^{GM}$, μ_{11}^{GM}, $\mu_0\mu_1^{GM}$	$\mu_0\mu_{15}^{GM}$, μ_{11}^{GM}, $\mu_0\mu_1^{GM}$	$\mu_0\mu_{15}^{GM}$, μ_{11}^{GM}, $\mu_0\mu_1^{GM}$
concentration	200 μg/mL	100 μg/mL	50 μg/mL
R^2	0.983	0.394	0.526
S	4.02	9.974	9.248
F	190.355	2.2	3.7
p	$<10^{-5}$	0.146	5.0×10^{-4}
q_{CV-LOO}^2	0.970	2.5	9.01

however, the model related with the percentage of the fungal growth inhibition at 200 μg/mL concentration is the best since it shows the best statistical values by describing 98.3% of the variance and with the greatest predictive capability of 97.0%.

Once the optimum condition of the concentration was selected to continue the QSAR study, we developed several models for the percentage of fungal growth inhibition at 200 μg/mL by changing the number of variables in every step of the analysis. In other words, once we developed a model, we calculated its statistical parameters and determined whether the introduction of the new variable into the model was justified. If it was, we compared the results with the previous models. We then repeated this analysis whenever a new variable was included. The first model contained two variables and was described with the following equation and the statistical parameters of the regression presented

$$\%GI = -52.38 \cdot \mu_0\mu_{15}^{GM} + 76.01 \cdot \mu_7^{GM} + 46.17 \quad (5)$$

where $N = 14$, $R^2 = 0.955$, $S = 6.193$, $F = 116.93$, $p < 10^{-5}$, $q_{CV-LOO}^2 = 0.927$, $S_{CV-LOO} = 7.877$, $q_{CV-LGO}^2 = 0.831$, and $S_{CV-LGO} = 9.214$ and where %GI is the percentage of the fungal growth inhibition and the parameters N, R^2, S, F, p, and q_{CV-LOO}^2 have been defined above. Also, we calculated the validation parameters shown previously, that is, cross-validated squared regression coefficient q^2 and the standard deviation Scv of the LOO and LGO procedures.

In this case, the statistic parameters quality was adequate. Nonetheless, we looked into the possibility of obtaining a new model with better statistical results and therefore introduced a new variable. The resulting model is shown below with its statistical parameters.

$$\%GI = 94.33 \cdot \mu_0\mu_{15}^{GM} - 58.71 \cdot \mu_{11}^{GM} + 21.43 \cdot \mu_0\mu_1^{GM} + 46.17 \quad (6)$$

where $N = 14$, $R^2 = 0.983$, $S = 4.02$, $F = 190.355$, $p < 10^{-5}$, $q_{CV-LOO}^2 = 0.970$, $S_{CV-LOO} = 5.267$, $q_{CV-LGO}^2 = 0.947$, and $S_{CV-LGO} = 6.971$.

As we had expected, the quality of statistic parameters improved by increasing the value of the R^2 (from 0.955 to 0.983) and of F (from 116.93 to 190.355) and by decreasing the value of S (from 6.193 to 4.02). The predictive capability of the model likewise was enhanced. This can be seen by the rise in cross-validation parameters, q_{LOO}^2 (from 0.927 to 0.970) and q_{LGO}^2 (from 0.0.831 to 0.947), and the fall in S_{LOO} (from 7.877 to 5.267) and for both procedures S_{LGO} (from 9.214 to 6.971).

However, in the specific case of the model containing four variables, the introduction of the new variable was not justified, as can be seen in the statistical parameters related to the following equation

$$\%GI = -71.54 \cdot \mu_{12}^{GM} + 126.02 \cdot \mu_0\mu_{12}^{GM} + 12.56 \cdot \mu_{14}^{Hyd} - 55.03 \cdot \mu_0\mu_1^{Mol} + 46.17 \quad (7)$$

where $N = 14$, $R^2 = 0.986$, $S = 3.745$, $F = 165.116$, $p < 10^{-5}$, $q_{CV-LOO}^2 = 0.959$, $S_{CV-LOO} = 6.548$, $q_{CV-LGO}^2 = 0.929$, and $S_{CV-LGO} = 7.801$.

Despite the relative improvement that certain parameters underwent, such as R^2, S, and F, the value of q_{LOO}^2 worsened (decrease from 0.970 to 0.959), along with q_{LGO}^2 (decrease from 0.947 to 0.929) as well as S_{LOO} (increase from 5.267 to 6.548) and S_{LGO} (increase from 6.971 to 7.801).

All things considered, we selected eq 6 as the best model because it features better statistical parameters than the model containing two variables and the greatest predictive capability with lower variability than the model described the eq 7.

In addition, a comparison between the model finally selected and another two models was developed with the same three variables for the inhibition growth percentage at the different concentrations 100 and 50 μg/mL. The results are given next.

As can be seen in Table 5, the variables considered as the best in the modeling at 200 μg/mL are not suitable to model the antifungal activity against *B. cinerea* at the other two concentrations. These variables are not well-correlated with the antifungal activity displayed by these compounds at 100 and 50 μg/mL concentrations, and it is worth noting that the concentration of the compounds tested might be related to their mechanism of action and the best weight for the variables is not necessarily the same for these concentrations.

The presence of outliers in QSAR models could lead to a degree of bias such that the model is unable to predict the "real" biological activity. Consequently, we looked for the presence of outliers in eq 6 but none were found because all of the compounds included in the training set had a standard residual value under $2 \cdot \delta$ where δ is equivalent to the standard deviation. However, another test was reserved for the analysis of deleted residual. In other words, the analysis of the residual value for every compound considered in this case was not included in the regression analysis. In this connection, we found that the deleted residual value of the compounds did not differ significantly from the respective standardized residual values, from which we deduced that there was not any outlier in the data set.

In addition, the analysis of the model domain of application (MDA) was carried out to find the applicability of the model and emphasize the absence of outliers. For this aim, the leverage values were calculated for every compound and plotted vs standard residuals (Y-axes). Then, the domain of applicability of the model is defined as a squared area within the ±2 band

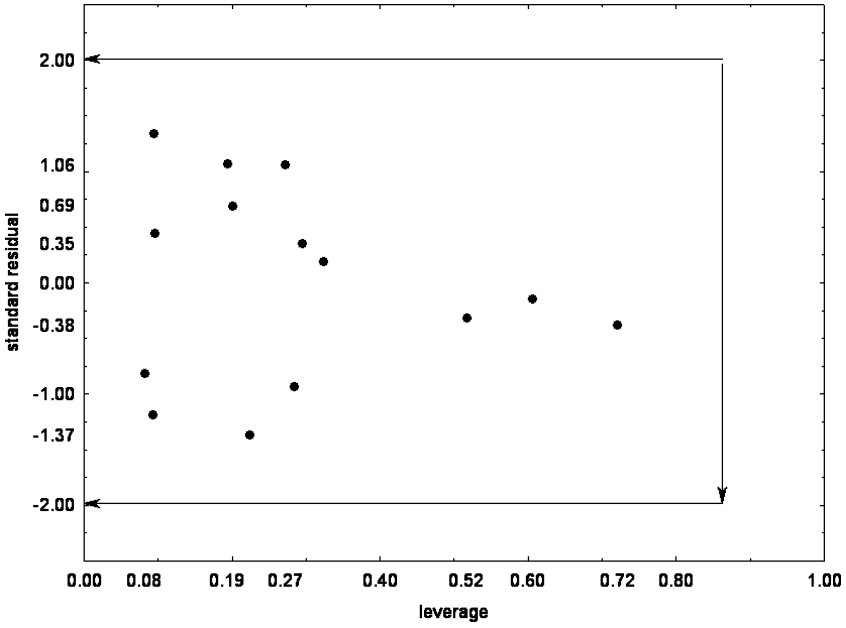

Figure 4. Model domain of application (MDA).

for residuals and a leverage threshold of $h = 0.857$ (*41*). The result of this study can be seen in the next table.

All compounds used in the training set lie within this area, and any outliers were detected as the previous analysis showed. Collinearity among variables was avoided by making an orthogonalization of molecular descriptors because interrelatedness among different descriptors can result in highly unstable models.

The QSAR model obtained with the spectral moments (eq 8) after orthogonalization and standardization is given below, together with the statistical parameters of regression analysis.

$$\%GI = 24.50 \cdot \Omega^1 \mu_0 \mu_{15}{}^{GM} + 7.65 \cdot \Omega^2 \mu_0 \mu_1{}^{GM} - 7.16 \cdot \Omega^3 \mu_{11}{}^{GM} + 46.17 \quad (8)$$

where $N = 14$, $R^2 = 0.983$, $S = 4.02$, $F = 190.355$, $p < 10^{-5}$, $q_{CV-LOO}{}^2 = 0.970$, $S_{CV-LOO} = 5.267$, $q_{CV-LGO}{}^2 = 0.947$, and $S_{CV-LGO} = 6.971$.

Once we obtained the definitive model, we developed an analysis of the bond contribution taking into account several fragments of the molecules and dividing the compounds into three groups to discover tendencies in the contributions made by these fragments to antifungal activity with the aim of extending the structure−activity relationship.

An analysis of bond contributions for the first compound set containing **2a**−**d** shows that the aromatic ring makes a positive contribution to biological activity and does not undergo significant modification by adding one electron-withdrawing substituent. This fact leads us to believe that low electron density at the aromatic ring does not tend to strengthen activity in this case. Another interesting fact is that while the molecular size of the substituent increases, the contribution of the ring decreases, possibly due to increasing difficulty in remaining on the same plane as the carbonyl group; therefore, the π electron overlap might decrease in these groups. This small decrease in activity might partly be counteracted by the incremental contribution of the substituents in ortho position, suggesting that an increase in the hydrophobicity either at that place or some other might increase the biological property (see **Figure 5**).

We also observed an interesting fact in the second set of compounds containing **3a**−**d**; while the property increases, as

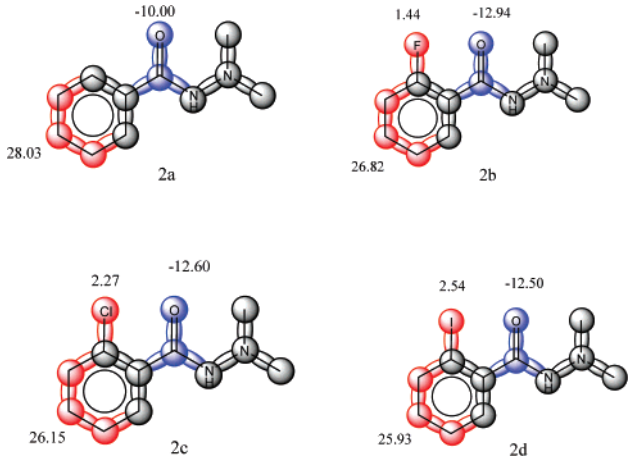

Figure 5. Structures of group number 1. Compounds **2a**–**d**. Fragments in blue have a negative contribution, and the red ones have a positive contribution.

explained above, as the number of aromatic rings rises, not all of these compounds affect it in a significant way (see compound **3a**). However, when a substituent in the ortho position is introduced in the benzoic acid, the contribution of this ring rises significantly whereas the others practically double their contributions. The reason for this could be that the inclusion of a substituent in this ring at the ortho position does not permit the rotation of the σ bond that exists between the ring and the carbonyl group as easily as in the absence of the substituent.

A postoptimization conformational analysis of the structures by the semiempiric PM_3 method shows that the ring in the **3a** compound may rotate 60° to one side or the other. It must cross an energy barrier with a maximum of 35 kcal/mol, until it comes up against barriers of higher energy content. These are difficult to overcome at the physiological temperature of any living organism, to be able to rotate bigger angles. Nevertheless, compounds **3b**, **3d**, and **3c** with chloride, methyl, and iodide in the ortho position must overcome a higher energy barrier for a rotation of only 25° in either direction. This rotation becomes increasingly difficult as the size of the substituent increases in this position **(Figure 6**). This could be because this planar system interacts more readily with certain proteins from a

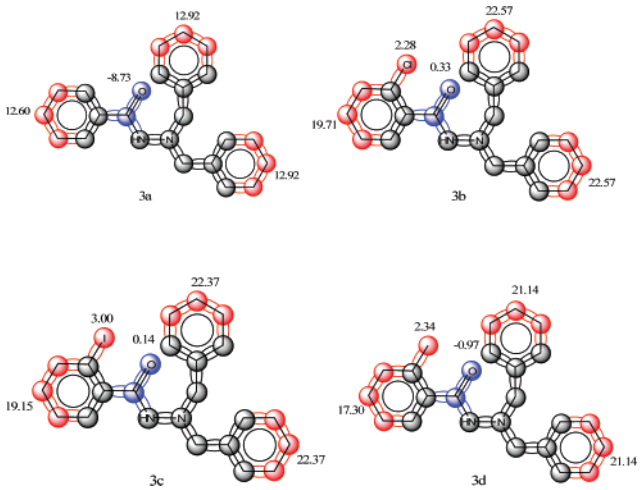

Figure 6. Contribution of fragments of compounds belonging to the second set. Compounds **3a**–**d**.

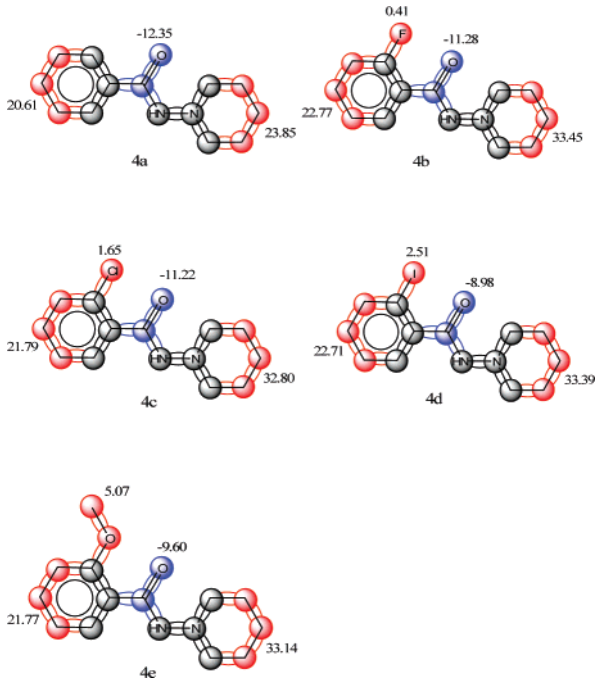

Figure 7. Contribution of fragments of compounds belonging to the third set. Compounds **4a**–**e**.

determined active place in the fungus, thus facilitating the latter's biotransformation and hence their antifungal effect due to a degree of rigidity in the molecules.

Analysis of the last set of compounds supports the previous explanation concerning aromatic ring contribution to biological properties. It shows the important role of hydrophobicity in the activity of these molecules due to the high contribution of the piperidine ring. This influence requires the presence of a hydrophobic substructure to enable the compound to cross the lipophobic or lipidic membranes of plants. They could therefore be considered more bioavailable in the exertion of their antifungal function.

A behavior similar to that observed in the previous sets is also observed when a substituent is introduced in the ortho position in the aromatic ring. The contribution of this substituent increases according to its size, and although in this case only a moderate increase in activity is achieved, it shows the importance of a second aromatic ring linked to the N of the hydrazine (**Figure 7**).

In summary, the activity displayed by the benzohydrazide derivatives studied here demonstrates that in addition to *N*′,*N*′-dibenzyl and *N*-aminoisoindoline substitution, the presence of a substituent in the ortho position of benzoic acid is critical to the antifungal activity of these molecules. On the other hand, while *N*′-benzyl substitution seems to play an important role in the inhibition mechanism by enhancing the antifungal activity of these compounds, the aliphatic chain on the nitrogen of benzohydrazide does not seem to have a significant effect on their fungistatic activity, except when the aliphatic chain is sufficiently large for it to be considered appropriately hydrophobic. Thus, the enhanced biological properties in that case (comparing the structures that only differ in the size of the aliphatic chain linked to nitrogen of the benzohydrazide) might be caused by the necessary balance provided by hydrophobicity to cross the lipophobic or lipidic membranes of plants. Work is under way to study the mode of action of these compounds on the metabolism of the fungus.

LITERATURE CITED

(1) Elad, Y., Williamson B., Tudzynsky, P., Delen, N., Eds. *Botrytis: Biology, Pathology and Control*; Kluwer Academic Publishers: Dordrecht, The Nertherlands, 2004.

(2) Kuhn, P. J. Mode action of carboximides. *Symp. Br. Mycol. Soc.* **1989**, *9*, 155−183.

(3) Pommer, E. H.; Zwick, W. Efficacy of systemic fungicides against Basidiomycetes. *Indian Phytopathol.* **1974**, *27*, 53−58.

(4) Kataria, H. R.; Verma, P. R.; Racow, G. Fungicidal control of damping-off and seedling root in Brassica species caused by *Rhizoctonia solani* in the growth chamber. *Ann. Appl. Biol.* **1993**, *123*, 247−256.

(5) Waisser, K.; Houngbedji, N.; Odlerova, Z.; Thiel, W.; Mayer, R. Tuberculostatics. Part 49. Thiohydrazides, potential tuberculostatics. *Pharmazie* **1990**, *45* (2), 141−142.

(6) Rando, D. G.; Sato, D. N.; Siqueira, L.; Malvezzi, A.; Leite, C. Q. F.; do Amaral, A. T.; Ferreira, E. I.; Tavares, L. C. Potential tuberculostatic agents. Topliss application on benzoic acid [(5-nitro-thiophen-2-yl)-methylene]-hydrazide series. *Bioorg. Med. Chem.* **2002**, *10*, 557−560.

(7) Eisa, H. M.; Tantawy, A. S.; El-Kerdawy, M. M. Synthesis of certain 2-aminoadamantane derivatives as potential antimicrobial agents. *Pharmazie* **1991**, *46*, 182−184.

(8) Parmar, S. S.; Gupta, A. K.; Gupta, T. K.; Stenberg, V. I. Synthesis of substituted benzylidinohydrazines and their monoamine oxidase inhibitory and anticonvulsant properties. *J. Pharm. Sci.* **1975**, *64*, 154−157.

(9) Thu-Cuc, N. T.; Buu-Hoy, N. P.; Xuong, N. D. Potential antifungal benzohydrazides. *Med. Pharm. Chem.* **1961**, *3*, 361.

(10) Akagi, T.; Mitani, S.; Komyoji, T.; Nagatani, K. Quantitative structure-activity relationships of fluazinam and related fungicidal N-phenylpyridinamines. Preventive activity against *Botrytis cinerea*. *Nippon Noyaku Gakkaishi* **1995**, *20* (3), 279−290.

(11) Akagi, T.; Mitani, S.; Ito, K.; Shigehara, I.; Komyoji, T.; Matsuo, N. Structure-activity relationships of pyridylcarbamates active against both benzimidazole-sensitive and -resistant isolates of *Botrytis cinerea*. *Pestic. Sci.* **1995**, *44* (1), 39−48.

(12) Humeres, E.; Cantos, G. A.; Debacher, N. A.; Nunes, R. J. Hydrophobicity constant of the dithiocarbamic fragment and QSAR of dithiocarbamate fungicides. *Org. React.* **1997**, *31* (1), 45−49.

(13) Kataoka, T. QSAR of 1-N-substituted azoles active against *Botrytis cinerea*. In *Rational Approaches to Structure, Activity and Ecotoxicology of Agrochemicals*; Draber, W., Fujita, T., Eds.; CRC: Boca Raton, FL, 1992; pp 465−482.

(14) González-Díaz, H.; Prado-Prado, F. J.; Santana, L.; Uriarte, E. Unify QSAR approach to antimicrobials. Part 1: Predicting antifungal activity against different species. *Bioorg. Med. Chem.* **2006**, *14*, 5973−5990.

(15) Arán, V. J.; Asensio, J. L.; Ruiz, J. R.; Stud, M. The heterocyclization of N′,N′-disubstituted 2-halobenzohydrazides to 1,1-disubstituted indazol-3-ylio oxides. *J. Chem. Res.* **1993**, 1322−1345.

(16) Noto, R.; Lamartina, L.; Arnone, C.; Spinelli, D. An analysis of carbon-13 NMR substituent chemical shifts in 3-substituted thiophene-2-carboxylic and 2-substituted benzoic acids by linear free energy relationships. *J. Chem. Soc. Perkin Trans.* **1988**, *2*, 887−892.

(17) Hönig, H. Improved 13C NMR shift prediction program for polysubstituted benzenes and sterically defined cyclohexane derivatives. *Magn. Reson. Chem.* **1996**, *34*, 395−406.

(18) Katritzky, A. R.; Rao, M. S. C. Chemistry of benzotriazole. Preparation of 1,1-disubstituted hydrazines and their 2-acyl derivatives. *J. Chem. Soc. Perkin Trans.* **1989**, *1*, 2297−2303.

(19) Katritzky, A. R.; Fan, W. Q. The chemistry of benzotriazole. A novel and versatile synthesis of 1-alkyl-, 1-aryl-, 1-(alkylamino)-, or 1-amido-substituted and of 1,2,6-trisubstituted piperidines from glutaraldehyde and primary amines or monosubstituted hydrazines. *J. Org. Chem.* **1990**, *55*, 3205−3209.

(20) Yeung, J. M.; Knaus, E. E. Synthesis of 3,6-dihydro-1(2H)-pyridinyl derivatives with hyperglycemic activity. *Eur. J. Med. Chem.—Chim. Ther.* **1986**, *21*, 181−185.

(21) Estrada, E. Spectral moments of the edge-adjacency matrix of molecular graphs. 2. Molecules containing heteroatoms and QSAR applications. *J. Chem. Inf. Comput. Sci.* **1997**, *37*, 320−328.

(22) Estrada, E. Spectral moments of the edge adjacency matrix in molecular graphs. 1. Definition and applications to the prediction of physical properties of alkanes. *J. Chem. Inf. Comput. Sci.* **1996**, *36*, 844−849.

(23) Estrada, E.; Uriarte, E.; Gutierrez, Y.; González, H. Quantitative structure-toxicity relationships using TOPS-MODE. 3. Structural factors influencing the permeability of commercial solvents through living human skin. *SAR QSAR Environ. Res.* **2003**, *14* (2), 145−163.

(24) Gutierrez, Y.; Estrada, E. *MODESLAB 1.0*; MOlecular DEScriptors LABoratory for Windows, 2002, http://www.modeslab.com.

(25) Statsoft, I. *STATISTICA (Data Analysis Software System)*, version 6.0; Statistica: 2002.

(26) Vedani, A.; Dobler, M. Multi-dimensional QSAR in drug research. Predicting binding affinities, toxicity and pharmacokinetic parameters. *Prog. Drug. Res.* **2000**, *55*, 105−35.

(27) Tropsha, A.; Zheng, W. Identification of the descriptor pharmacophores using variable selection QSAR: Applications to database mining. *Curr. Pharm. Des.* **2001**, *7* (7), 599−612.

(28) Hasegawa, K.; Funatsu, K. Partial least squares modeling and genetic algorithm optimization in quantitative structure-activity relationships. *SAR QSAR Environ. Res.* **2000**, *11* (3−4), 189−209.

(29) Klein, D. J.; Randić, M.; Babić, D.; Lučić, B.; Nikolić, S.; Trinajstić, N. Hierarchical orthogonalization of descriptors. *Int. J. Quantum Chem.* **1991**, *63* (1), 215−222.

(30) Randić, M. Correlation of enthalphy of octanes with orthogonal connectivity indices. *J. Mol. Struct. (Theochem)* **1991**, *233*, 45−59.

(31) Randić, M. Orthogonal molecular descriptors. *New J. Chem.* **1991**, *15* (7), 517−525.

(32) Randić, M. Resolution of ambiguities in structure-property studies by use of orthogonal descriptors. *J. Chem. Inf. Comput. Sci.* **1991**, *31*, 311−320.

(33) Lučić, B.; Nikolić, S.; Trinajstić, N.; Jurić, D. The structure-property models can be improved using the orthogonalized descriptors. *J. Chem. Inf. Comput. Sci.* **1995**, *35*, 532−538.

(34) Hawkins, D. M. The problem of overfitting. *J. Chem. Inf. Comput. Sci.* **2004**, *44* (1), 1−12.

(35) Estrada, E.; Patlewicz, G.; Gutierrez, Y. From knowledge generation to knowledge archive. A general strategy using TOPS-MODE with DEREK to formulate new alerts for skin sensitization. *J. Chem. Inf. Comput. Sci.* **2004**, *44* (2), 688−98.

(36) González, M. P.; Teran, C.; Teijeira, M. A topological function based on spectral moments for predicting affinity toward A_3 adenosine receptors. *Bioorg. Med. Chem. Lett.* **2006**, *16*, 1291−1296.

(37) Anthoni, U.; Larsen, C.; Nielsen, P. H. Derivatives of hydrazine. V. Cis-trans isomerism, dipolar structure, and magnetic nonequivalence of the isopropyl methyl 1H NMR signals of acyl and thioacyl N,N-diisopropylhydrazines. *Acta Chem. Scand.* **1969**, *23*, 3513−3524.

(38) Walter, W.; Reubke, K. J. Structure of N,N-dialkylhydrazides. *Chem. Ber.* **1970**, *103*, 2197−2207.

(39) Dewar, M. J. S.; Jennings, W. B. Conformational interchange in acyclic hydrazines. *J. Am. Chem. Soc.* **1973**, *95*, 1562−1569.

(40) Golbraikh, A.; Tropsha, A. Beware of q2! *J. Mol. Graphics Modell.* **2002**, *20* (4), 269−276.

(41) Gonzalez-Díaz, H.; Vilar, S.; Santana, L.; Uriarte, E. On the applicability of QSAR for recognition of miRNA bioorganic structures at early stages of organism and cell development: Embryo and stem cells. *Bioorg. Med. Chem.* **2007**, *15*, 2544−2550.

Received for review February 13, 2007. Revised manuscript received April 12, 2007. Accepted April 12, 2007. Financial support from the Spanish Science and Technology Ministery through project AGL2006-13401-C02-01 is gratefully acknowledged.

JF0704211